Article citation info:
KOLAKOWSKI Z, MANIA RJ, GRUDZIECKI J. Local nonsymmetrical postbuckling equilibrium path of the thin FGM plate. Eksploatacja i Niezawodnosc – Maintenance and Reliability 2015; 17 (1): 135–142.

Zbigniew KOLAKOWSKI
Radosław J. MANIA
Jan GRUDZIECKI

LOCAL NONSYMMETRICAL POSTBUCKLING EQUILIBRIUM PATH OF THE THIN FGM PLATE

NIESYMETRYCZNA LOKALNA ŚCIEŻKA RÓWNOWAGI POKRYTYCZNEJ CIENKIEJ PŁYTY Z MATERIAŁU FUNKCJONALNIE GRADIENTOWEGO

The influence of the imperfection sign (sense) on local postbuckling equilibrium path of plates made of functionally graded materials (FGMs) has been analyzed. Koiter's theory has been used to explain this phenomenon. In the case of local buckling, a nonsymmetrical stable equilibrium path has been obtained. The investigations focus on a comparison of the semi-analytical method (SAM) and the finite element method (FEM) applied to the postbuckling nonlinear analysis of thin-walled complex FG plated structures.

***Keywords**: FGM, FEM, Koiter's theory, semi-analytical method, postbuckling path.*

W pracy przedstawiono analizę wpływu znaku imperfekcji wstępnej na charakterystykę lokalnej pokrytycznej ścieżki równowagi płyty wykonanej z materiału gradientowego. Do wyjaśnienia tego efektu zastosowano teorię Koitera. W przypadku lokalnej utraty stateczności uzyskano niesymetryczne stateczne ścieżki równowagi. Prezentowane badania były skoncentrowane na porównaniu wyników uzyskanych na podstawie własnej metody pół-analitycznej z wynikami uzyskanymi przy zastosowaniu metody elementów skończonych w nieliniowej analizie cienkościennych konstrukcji płytowych wykonanych z materiałów gradientowych.

***Słowa kluczowe**: materiały funkcjonalnie gradientowe, MES, teoria Koitera, metoda pól-analityczna, ścieżka pokrytyczna.*

1. Introduction

Since the mid 1980's Functionally Graded Materials (FGMs) have been a relatively new class of composite materials, which have become a very popular research field and have been used in numerous engineering applications. A standard functionally gradient material is an inhomogeneous composite made up of two constituents – typically of metallic and ceramic phases. Within FGMs, different microstructural phases have different functions, and the overall FGMs attain the multistructural status from their property gradation. In most cases, these phases content changes gradually along the thickness of the plate or shell. This eliminates adverse effects between the layers (e.g., shear stress concentrations and/or thermal stress concentrations), typical for layered composites what generally improves material utility properties. The combination of ceramic with a metal component improves the characteristics of FGM structures i.e. a better resistance to high temperature (ceramic) and good mechanical features (metal), reducing further a fracture possibility of the whole gradient structure. These features make high temperature environments the leading application area of FGM structures.

The nonlinear analysis of plates and shells devoted to basic types of loads is covered in the monograph by Hui-Shen [4]. Author considers static bending and thermal bending as an introduction to buckling and postbuckling behaviour of FGM plates and shells. The shear deformation effect is employed in the framework of Reddy's higher order shear deformation theory (HSDT) [20].

In [19], alongside the HSDT for FGM plates, Reddy compares the application of the first order shear deformation theory (FSDT) and the classical laminated plate theory (CLPT) to functionally graded plate analysis. According to the presented results for thin-walled plates, it is obvious that an application of the FSDT gives practically the same results as the HSDT. The discrepancy between both theories is of 2% in the calculated deflections of the plates under analysis.

The buckling problem of functionally graded plates is discussed in the frame of different approaches and for different loads: in [21] - biaxial in-plane compression; thermal loads (constant temperature) with axial compression in [24]; biaxial in-plane compression in [2] and [16], and through the thickness temperature gradient in [23].

Birman and Byrd [1] give a wide review of theories employed for a description of grading material properties and focus on the principal developments in functionally graded materials (FGMs) with an emphasis on the recent works published since 2000 (up to 300 works cited).

In some papers (e.g.,[14, 27]), the concept of 'physical neutral surface' that allows one to uncouple the in-plane and out-of-plane deformations is introduced.

Due to the complexity of buckling problems of FG plates under compound mechanical and thermal loads, the finite element method (FEM) seams to be the only possible solution in many cases. Therefore, in the literature one can find many papers which present results of a solution to different problems of FG plate buckling, obtained with an application of the FEM, for example [15, 17, 22].

In current paper in the finite element method solution, FG plates were modelled as multilayered composite structures whose graded material properties in the range of 10–40 isotropic layers were defined. After the convergence analysis the model with twenty layers

was accepted. For meshing, a shell element with four nodes and six degrees of freedom in each node was employed. The rotational DOF in the plane of the element was constrained via the penalty function.

Conducting with the FEM the nonlinear buckling analysis of a rectangular FGM plate, subjected to one-directional compression in its plane, the authors of the present paper have observed some intriguing influence of the imperfection sign (i.e., its direction) on postbuckling equilibrium paths of investigated FGM plates. Therefore, this work is aimed at an explanation of this phenomenon. The general asymptotic Koiter's theory of stability has been assumed as the basis of investigation. Among all versions of the general nonlinear theory, Koiter's theory [6, 7, 25, 26] of conservative systems is the most popular one, owing to its general character and development. Even more, so after Byskov and Hutchinson [3] formulated it in a convenient way. The theory is based on asymptotic expansions of the postbuckling path for potential energy of the system.

The nonlinear stability of thin-walled multilayer structures in the first order approximation of Koiter's theory is solved with the modified analytical-numerical method (ANM) presented in [8]. The analytical-numerical method (ANM) should also consider the second order approximation in the postbuckling analysis of elastic composite structures. The second order postbuckling coefficients were estimated with the semi-analytical method (SAM) [12], modified by the solution method given in [11]. The investigation of stability of equilibrium states requires an application of a nonlinear theory that enables us to estimate an influence of different factors on the structure behaviour. The analysis of postbuckling behaviour of thin-walled composite plate structures using the SAM will be by far faster and more thorough than the FEM.

The initial imperfections were introduced by updating the finite element mesh with the first mode shape of the eigen-buckling solution, with a given magnitude corresponding to the plate thickness and assumed sign (direction). The eigen-buckling analysis, where the critical load was determined despite the eigen-mode, preceded the nonlinear buckling analysis.

2. Formulation of the problem

The square plate is supported at all their edges. It is assumed that the FG plate obeys Hooke's law. The material properties are assumed to be temperature independent.

In strain-displacement relations - in order to enable the consideration of both out-of-plane and in-plane bending of the plate, all nonlinear terms are present [8, 9, 11]:

$$\begin{aligned}\varepsilon_x &= u_{,x} + \tfrac{1}{2}\ (w_{,x}^2 + v_{,x}^2 + u_{,x}^2)\\ \varepsilon_y &= v_{,y} + \tfrac{1}{2}\ (w_{,y}^2 + u_{,y}^2 + v_{,y}^2)\\ 2\varepsilon_{xy} &= \gamma_{xy} = u_{,y} + v_{,x} + w_{,x}w_{,y} + u_{,x}u_{,y} + v_{,x}v_{,y}\end{aligned} \tag{1}$$

and

$$\kappa_x = -w_{,xx} \qquad \kappa_y = -w_{,yy} \qquad \kappa_{xy} = -2w_{,xy} \tag{2}$$

where: u, v, w – are components of the displacement vector of the plate in the x, y, z axis direction, respectively, and the plane $x-y$ overlaps the midplane before its buckling.

It should be highlighted that in the majority of publications devoted to stability of structures, the terms $(v_{,x}^2 + u_{,x}^2)$, $(u_{,y}^2 + v_{,y}^2)$ and $(u_{,x}u_{,y} + v_{,x}v_{,y})$ in strain tensor components (1) are neglected. However, the main limitation of the assumed theory lies in an assumption of linear relationships between curvatures (2) and second derivatives of the displacement w. In such an approach, finite displacements and small or moderate rotations are considered [11].

In thin-walled FG structures - plates or shells, usually the ceramic volume fraction V_c and metal fraction V_m distribution throughout the structure thickness t are described by a simple power law of:

$$V_c(z) = \left(\frac{z}{t} + \frac{1}{2}\right)^q \qquad V_m(z) = 1 - V_c(z) \tag{3}$$

where: $-t/2 \le z \le t/2$ and $q \ge 0$ is the volume fraction exponent (i.e., for $q = 0$ – plate is full ceramic and for $q = \infty$ – plate is metallic – see Fig. 1).

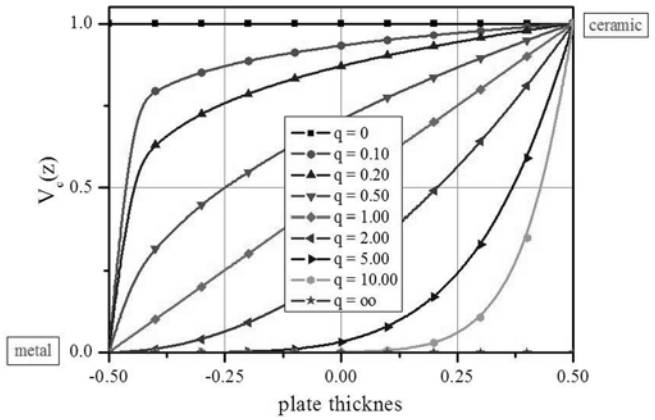

Fig. 1. Volume fraction of ceramic along the FGM plate thickness

According to the rule of mixture, the properties of the functionally graded material (E – Young's modulus, ν – Poisson's ratio etc.) can be expressed as follows:

$$\begin{aligned}E(z) &= E_m + (E_c - E_m)\left(\frac{z}{t} + \frac{1}{2}\right)^q\\ \nu(z) &= \nu_m + (\nu_c - \nu_m)\left(\frac{z}{t} + \frac{1}{2}\right)^q\end{aligned} \tag{4}$$

In the present study, the classical plate theory is employed to obtain the governing equations of the thin FG plate equilibrium. Using the classical laminated plate theory (CLPT), the stress and moment resultants (N, M) are defined as [5, 8, 9]:

$$\begin{Bmatrix} N \\ M \end{Bmatrix} = \begin{bmatrix} A & B \\ B & D \end{bmatrix} \begin{Bmatrix} \varepsilon \\ \kappa \end{Bmatrix} \tag{5}$$

where: A, B, D – are extensional, coupling and bending stiffness matrices, respectively. For the FG plate their components are listed below:

$$\begin{aligned}A_{11} = A_{22} &= \int_{-t/2}^{t/2} \frac{E(z)}{1-\nu^2(z)}\, dz\\ A_{12} = A_{21} &= \int_{-t/2}^{t/2} \frac{E(z)\nu(z)}{1-\nu^2(z)}\, dz\end{aligned} \tag{6a}$$

$$A_{66} = \int_{-t/2}^{t/2} \frac{E(z)}{2[1+\nu(z)]}\, dz$$

$$A_{16} = A_{61} = 0$$

$$B_{11} = B_{22} = \int_{-t/2}^{t/2} \frac{E(z)}{1-\nu^2(z)}\, zdz$$

$$B_{12} = B_{21} = \int_{-t/2}^{t/2} \frac{E(z)\nu(z)}{1-\nu^2(z)}\, zdz \tag{6b}$$

$$B_{66} = \int_{-t/2}^{t/2} \frac{E(z)}{2[1+\nu(z)]}\, zdz$$

$$B_{16} = B_{61} = 0$$

$$D_{11} = D_{22} = \int_{-t/2}^{t/2} \frac{E(z)}{1-\nu^2(z)}\, z^2dz$$

$$D_{12} = D_{21} = \int_{-t/2}^{t/2} \frac{E(z)\nu(z)}{1-\nu^2(z)}\, z^2dz \tag{6c}$$

$$D_{66} = \int_{-t/2}^{t/2} \frac{E(z)}{2[1+\nu(z)]}\, z^2dz$$

$$D_{16} = D_{61} = 0$$

and

$$\{\varepsilon\} = \begin{Bmatrix} \varepsilon_x \\ \varepsilon_y \\ 2\varepsilon_{xy} \end{Bmatrix} \quad \{\kappa\} = \begin{Bmatrix} \kappa_x \\ \kappa_y \\ \kappa_{xy} \end{Bmatrix} \tag{7}$$

Due to the presence of the nontrivial submatrix B, the coupling between extensional and bending deformations exists as it is in the case of unsymmetrical laminated plates [5, 8, 9]. An extensional force results not only in extensional deformations, but also bending of the FG plate. Moreover, such a plate cannot be subjected to the moment without suffering simultaneously from extension of the middle surface. Coupling between extension and bending is a result of a combination of the geometry and FGM properties in the structures. The stretching-bending coupling affects strongly the constitutive equations and the boundary conditions that have a complex form and the solution procedures become difficult.

The equations of stability of thin-walled structures have been derived using a variational method [8, 9, 11]. After expanding the fields of displacements $\bar{U}$ and the fields of sectional forces $\bar{N}$ into a power series with respect to the mode amplitudes ζ_1 (the dimensionless amplitude of the buckling mode), Koiter's asymptotic theory has been employed [3, 6, 7, 8, 9, 10, 13, 18, 25, 26]:

$$\begin{aligned} \bar{U} &= \lambda\bar{U}^{(0)} + \zeta_1\bar{U}^{(1)} + \zeta_1^2\bar{U}^{(2)} + ... \\ \bar{N} &= \lambda\bar{N}^{(0)} + \zeta_1\bar{N}^{(1)} + \zeta_1^2\bar{N}^{(2)} + ... \end{aligned} \tag{8}$$

where: λ – load parameter, $\bar{U}^{(0)}$, $\bar{N}^{(0)}$ – prebuckling state fields (the zero approximation), $\bar{U}^{(1)}$, $\bar{N}^{(1)}$ – buckling mode fields (the first order approximation), and $\bar{U}^{(2)}$, $\bar{N}^{(2)}$ – postbuckling fields (the second order approximation) for the structure.

The postbuckling equilibrium path within an imperfect structure with the amplitude ζ_1^* for the single mode (i.e., an uncoupled mode), buckling mode has the following form [3, 8, 9, 13, 26]:

$$a_1\left(1-\frac{\sigma}{\sigma_{cr}}\right)\zeta_1 + a_{111}\zeta_1^2 + a_{1111}\zeta_1^3 + ... = a_1\frac{\sigma}{\sigma_{cr}}\zeta_1^* \tag{9}$$

where: σ_{cr} – critical (bifurcational) value of σ (instead of λ). The coefficients in equilibrium equation (9) are given in papers [3, 8, 9, 13, 26]. It can be easily seen that the amplitude ζ_1^* is a small quantity (i.e., only linear terms with respect to ζ_1^* have been accounted for) and the linear pre-buckling state is assumed.

The corresponding expression for the total elastic potential energy of the structure has the following form:

$$\Pi = -a_0\frac{\sigma^2}{2} + a_1\left(1-\frac{\sigma}{\sigma_{cr}}\right)\frac{\zeta_1^2}{2} + a_{111}\frac{\zeta_1^3}{3} + a_{1111}\frac{\zeta_1^4}{4} - a_1\frac{\sigma}{\sigma_{cr}}\zeta_1\zeta_1^* \tag{10}$$

where: $\Pi_0 = a_0\frac{\sigma^2}{2}$ is energy of the prebuckling linear state.

In the semi-analytical method (SAM), one postulates to determine approximated values of the a_{1111} coefficients on the basis of the linear buckling problem. This approach allows the values of the a_{111} coefficients - according to the applied nonlinear Byskov and Hutchinson theory [3, 8, 9, 13, 26] – to be precisely determined.

The considerations performed in [12] and the results of [11] allow for concluding that the approximated values of the a_{1111} coefficients correspond to an application of the following simple supported boundary conditions of the plate at both edges (i.e. $x = 0; \ell$)

$$\begin{aligned} &\int_0^b N_x(x=0,y)dy = \int_0^b N_x(x=\ell,y)dy = bN_x^{(0)} \\ &v(x=0,y) = v(x=\ell,y) = 0 \\ &w(x=0,y) = w(x=\ell,y) = 0 \\ &M_x(x=0,y) = M_x(x=\ell,y) = 0 \end{aligned} \tag{11}$$

The first condition in (11) means that the external loading is not subjected to any additional increment.

At the critical point, the dependence describing the relationship for the ideal structure (i.e., without the imperfection $\zeta_1^* = 0$) is subject to bifurcation between the external loading and the displacement amplitude ζ_1. Equilibrium path equation (9) can be treated as the first variation of the system potential energy, that is to say, as the condition necessary for the system equilibrium. For the case when the postbuckling coefficients $\bar{a}_{111} = a_{111}/a_1 \neq 0$ and $\bar{a}_{1111} = a_{1111}/a_1 > 0$ (which corresponds to the case of the FGM plate), in order to determine the

equilibrium state, the second variation of energy was calculated Then the intersection points of the equilibrium path and the structure stability limit of the ideal structure were determined. Finally, the coordinates of two points $p1, p2$ were arrived at:

$$\zeta_{p1} = 0 \quad \left(\frac{\sigma}{\sigma_{cr}}\right)_{p1} = 1 \tag{12}$$

$$\zeta_{p2} = -\frac{\bar{a}_{111}}{2\bar{a}_{1111}} \quad \left(\frac{\sigma}{\sigma_{cr}}\right)_{p1} = 1 - \frac{\bar{a}_{111}^2}{4\bar{a}_{1111}} \tag{13}$$

A sample equilibrium path for the ideal square FGM plate is presented in Fig. 2. There it is visible that in the case of the FG plate, an nonsymmetrical stable equilibrium path exists. The unstable configuration corresponds to the postbifurcational equilibrium path of the plate without imperfection in the range $<\zeta_{p1}, \zeta_{p2}>$.

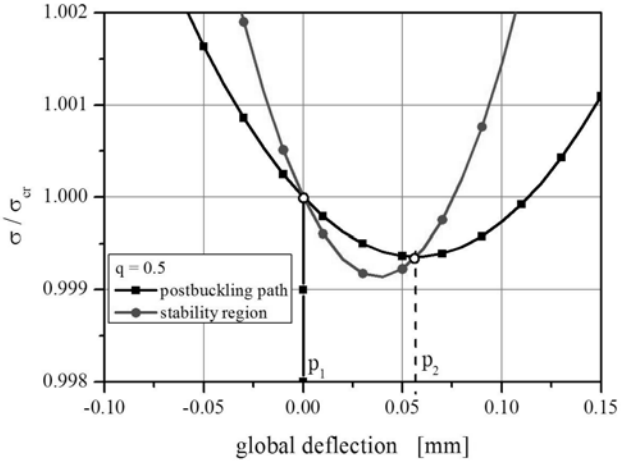

Fig. 2. Postbuckling path of FGM plate

In the linear problem, the critical stress σ_{cr} is the characteristic quantity, whereas in the nonlinear first order problem, the magnitude of the coefficient $\bar{a}_{111}$ determining the sensitivity to imperfections should be accounted for.

3. Analysis of the results

Detailed numerical computations were conducted only for a square FGM plate. The plate is subjected to uniform compression in the direction of *x* axis. All plate edges are assumed to be simply supported. Although, in the subsection devoted to determination of critical stress, some other boundary conditions along the unloaded edges are considered as well.

The following geometrical dimensions of the square plate (Fig. 3) and the material constants for Al-TiC are assumed:

$\ell = b = 100$ mm; $t = 1$ mm; $E_m = 69$ GPa; $\nu_m = 0.33$; $E_c = 480$ GPa; $\nu_c = 0.2$.

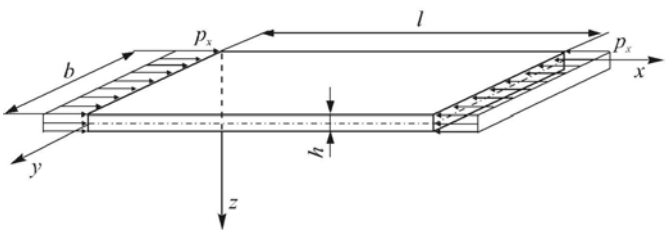

Fig. 3. Geometry and loading of FGM plate

where: indices *m* and *c* refer to the metal (Al) and ceramic material (TiC), respectively.

In [8], an unbending, prebuckling state, i.e., a distribution field of the zero state according to (A1) has been assumed. According to assumed (A1) and (8) displacements, for the zero state (i.e., prebuckling) the force and moment dependence (5) takes the form:

$$\begin{Bmatrix} N^{(0)} \\ M^{(0)} \end{Bmatrix} = \begin{bmatrix} A & B \\ B & D \end{bmatrix} \begin{Bmatrix} \varepsilon^{(0)} \\ 0 \end{Bmatrix} \tag{14}$$

Then for the zero state, it results in an occurrence of nonzero inner sectional forces (A2) $N_x^{(0)}$, $M_x^{(0)}$, $M_y^{(0)}$ in the FG plate. Special attention should be drawn to the fact that nonzero magnitudes of the sectional moments $M_x^{(0)}$ and $M_y^{(0)}$ appear as the effect of the middle surface deformations (i.e., membrane deformations) and the nontrivial coupling submatrix B but not due to an appearance of the middle surface curvatures. These moments affect the values of critical loads and the values of postbuckling coefficients.

In the subsequent three figures (Figs. 4 - 6), an effect of the volume fraction exponent q in Eq. (3), on the values of critical stresses and the postbuckling coefficients $\bar{a}_{111}$ and $\bar{a}_{1111}$ for various constrain cases of unloaded longitudinal edges, i.e., $y = 0; b$, is presented. In legends to these figures the descriptions mean:

- F – free edges, for which the following has been assumed: $N_y = N_{xy} = M_y = Q_y = 0$;
- S1 – simply supported edges - $N_y = N_{xy} = w = M_y = 0$;
- S2 – simply supported edges - $v = N_{xy} = w = M_y = 0$;
- C – clamped edges - $N_y = N_{xy} = w = \partial w / \partial y = 0$.

In the case of clamped longitudinal edges $(y = 0; b)$, the same results have been obtained as for two other possible conditions of the edge support, i.e., when:

- $v = N_{xy} = w = \partial w / \partial y = 0$
- $u = v = w = \partial w / \partial y = 0$

The values of critical loads (Fig. 4) for the boundary conditions under consideration increase with a decrease in the values of volume fractions q – as can be expected. Differences in the values of critical loads for cases S1 and S2 become visible for $q > 0.5$. They are relatively inconsiderable (below 10%) and larger for case S2.

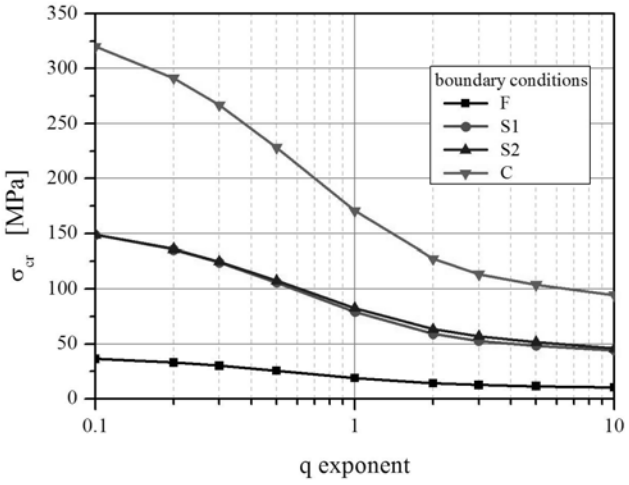

Fig. 4. Dependence of critical stress on boundary conditions and q factor

In the range $0.1 \le q \le 10$, the values of postbuckling coefficients $\bar{a}_{111}$ (Fig. 5) are negative for all considered cases of boundary conditions. The lowest values occur for case F, whereas for clamped conditions C, they are located between values for S1 and S2. The highest values have been found for boundary conditions S2. The maximal values of $\bar{a}_{111}$ for the analyzed support conditions are reached for $2 \le q \le 3$.

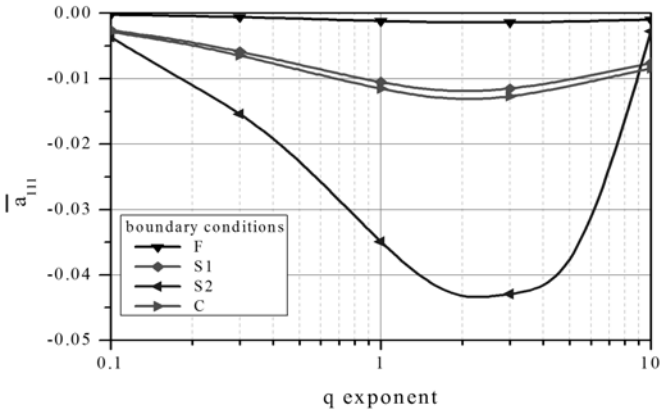

Fig. 5. Coefficient $\bar{a}_{111}$ value as a function of q and boundary conditions

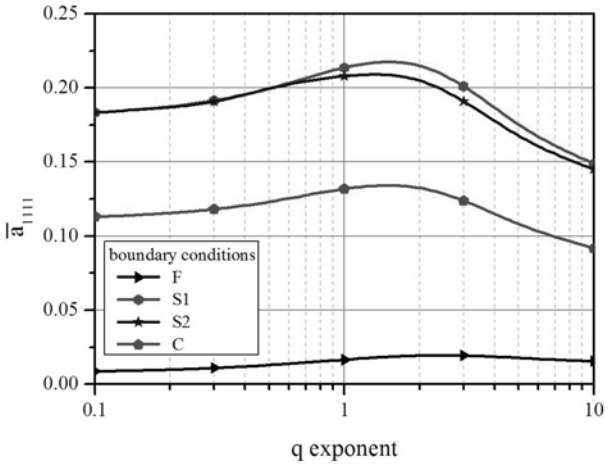

Fig. 6. Coefficient $\bar{a}_{1111}$ value as a function of q and boundary conditions

On the other hand, the values of postbuckling coefficients $\bar{a}_{1111}$ (determined according to the SAM [11, 12]), shown in Fig. 6, are positive for the assumed boundary conditions F, S1, S2, C for $0.1 \le q \le 10$. The lowest values of $\bar{a}_{1111}$ have been obtained, as expected, for case F. The values of $\bar{a}_{1111}$ for case C are by approximately 60% lower than for conditions S1 and S2. For condition S2, the values of $\bar{a}_{1111}$ are higher than for S1, and these differences become visible for $q > 0.5$. However, they do not exceed 5% for the range of variability $0.1 \le q \le 10$ under consideration.

As it has been discussed in detail in [8], sectional moments of the zero state $M_x^{(0)}$ and $M_y^{(0)}$ do not enter the first order equations of equilibrium and boundary conditions. The nonzero values of postbuckling three-index coefficients $\bar{a}_{111}$ result from an occurrence of the nonzero coupling submatrix B. The coefficient $\bar{a}_{111}$ characterizing the initial postbuckling behaviour belongs to surface integrals of the type $\sigma^{(1)} \cdot l_2(U^{(1)})$ (according to the notation introduced by Byskov and Hutchinson [3, 26]). An appearance of first order internal forces (i.e., related to the forces $N_x^{(1)}, N_y^{(1)}, N_{xy}^{(1)}$) causes that the coefficients $\bar{a}_{111}$ reach values other than zero. It should be noted yet that the values of $\bar{a}_{111}$, in principle, are relatively small. Due to the above-mentioned reasons, in the analysis of postbuckling equilibrium paths of the FG plate they have been usually neglected. However, when we take into account the nonzero values of $\bar{a}_{111}$, a phenomenon of occurrence various postbuckling equilibrium paths for different signs of imperfection (i.e., $\left|\zeta_1^*\right|$) can be explained. Due to the boundary conditions (11) assumed along the loaded edges ($x = O; \ell$) and unloaded edges ($y = O; b$) - respectively for cases F, S1, S2, and C; one obtains different distributions of inner forces of the first order, i.e., $N_x^{(1)}, N_y^{(1)}, N_{xy}^{(1)}, M_x^{(1)}, M_y^{(1)}, M_{xy}^{(1)}$. These inner forces values are determined with accuracy up to a constant, as it takes place for eigenproblems. The conditions on loaded edges (11a) enforce a generation of a self-balancing system of forces $N_x^{(1)}$. Below, few exemplary diagrams for S2 boundary conditions on longitudinal edges, for $q = 0.5$ are shown.

In Fig.7, distributions of first-order inner membrane forces $N_x^{(1)}, N_y^{(1)}, N_{xy}^{(1)}$ are shown, whereas the corresponding distributions of bending moments $M_x^{(1)}, M_y^{(1)}, M_{xy}^{(1)}$ along the plate width are additionally presented in Fig. 8. As it can be easily noticed, the values of inner forces are of the same order of magnitude. According to the assumption, the distributions of inner forces $N_x^{(1)}, N_y^{(1)}, M_x^{(1)}, M_y^{(1)}$ are symmetrical with respect to the plate axis of symmetry (i.e., for $y = O.5b$), whereas the distribution of $N_{xy}^{(1)}, M_{xy}^{(1)}$ forces is antisymmetrical. The boundary conditions of unloaded edges cause a self-resetting of $N_{xy}^{(1)}, M_y^{(1)}$. For edges $y = O; b$ the value of moment $M_x^{(1)}$ is other than zero and results from the first-order nonzero membrane deformations $\varepsilon_x^{(1)}, \varepsilon_y^{(1)}$ and the nontrivial coupling matrix B. The nonzero values of all first-order inner forces for the FGM plate cause that nonzero values of the coefficients $\bar{a}_{111}$ appear. These values are relatively low but exert a significant effect on the sensitivity of the system to values and signs of the imperfection ζ_1^*.

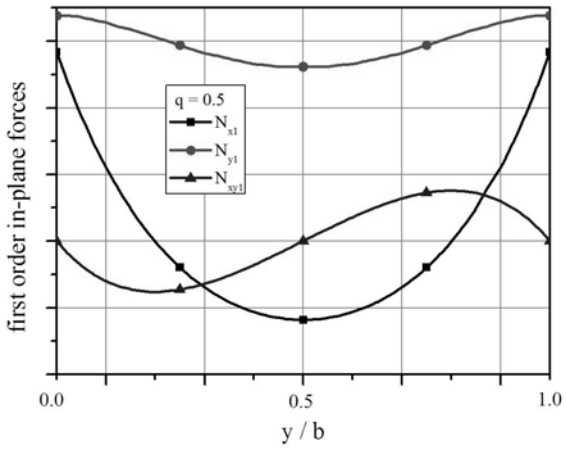

Fig. 7. First order in-plane force resultants distribution along the plate width

To verify the proposed SAM solution, finite element computations were performed for the FG plate under axial loading. The commercial ANSYS software was applied for the numerical calculations.

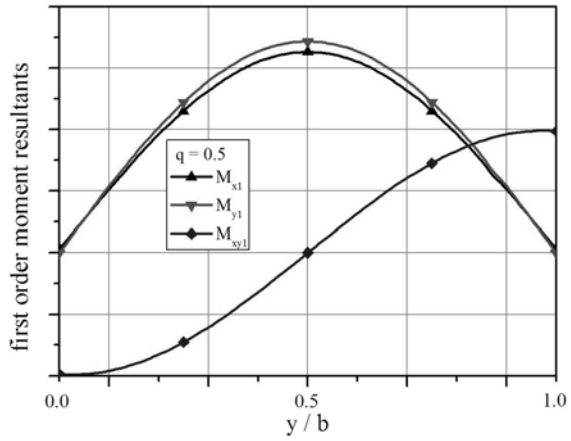

Fig. 8. First order moment resultants distribution along the plate width

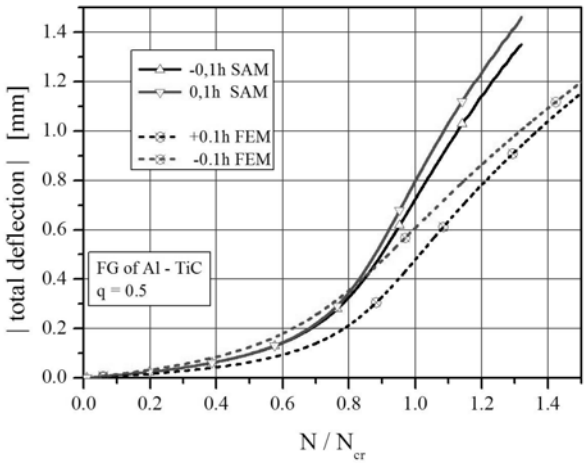

Fig. 9. Sign of imperfection influence on the buckling and postbuckling path

The numerical model was created with an application of a shell finite element. It was a multi-layered four-node element with six degrees of freedom at each node (three translations in the directions of local coordinate axes and three rotations around these axes). The rotational DOF around the normal to the plate midplane was constrained via the penalty function to relate this independent rotation with the in-plane components of displacements. This element is dedicated for modelling multi-layered structures and is equipped with the section option which allows for easy tailoring the lay-ups of the modelled plate. The sensitivity to shear strains in this element is governed by the first-order shear deformation theory, whereas the element formulation is based on the logarithmic strain measure. According to the current analysis requirements, the applied finite element was associated with linear elastic material properties. To discretize the model, a uniform mesh of elements was generated. The boundary conditions on loaded plate edges, which followed from S1 type analytical simple support, were introduced by displacement constrains in appropriate directions as well as coupling of edge node displacements to keep the edges straight.

The initial imperfection was introduced by updating the finite element mesh with the local mode shape of the eigen-buckling solution, with a given magnitude corresponding to the plate thickness. The eigen-buckling analysis, where the critical load was determined despite the eigen-mode, preceded the nonlinear analysis. Therefore, the numerical model employed large displacement formulation. The load was applied to the plate edges in the form of uniformly distributed node forces.

For the square plate under analysis and for $q = 0.5$, the results of calculations obtained from the SAM and the FEM were compared. A comparison of the results is presented in Fig. 9. For an easier comparison of an influence of the imperfection ζ_1^* sign, a change in the absolute values of total deflections $|w_t| = |w_0 + w| = |\zeta_{1t}| \;\; t = \left|\zeta_1^* + \zeta_1\right| \;\; t$ as a function of the load ratio $N / N_{cr} = \sigma / \sigma_{cr}$ has been shown. The negative value of imperfection corresponds to a initial deflection along the direction of metal, whereas the positive one - along the direction of ceramic.

The results obtained with the FEM are achieved for a full geometrically nonlinear analysis. On the other hand, in the SAM, nonlinear terms related to the imperfection ζ_1^* were neglected, whereas the values of the postbuckling coefficient $\overline{a}_{1111}$ were determined approximately. It is followed by visible differences in the results obtained with both the methods (SAM and FEM) for the same value of imperfection. It can be seen that the sign of imperfection exerts an influence on the postbuckling equilibrium path. The initial deflection ζ_1^* along ceramic yields higher values of total deflections for the given value of load N / N_{cr} than the initial deflection along the direction of metal. In both cases the assumed absolute value of imperfection $\left|\zeta_1^*\right|$ was equal.

Thus, as it was discussed above, the application of Koiter's theory through the semi-analytical method enables an explanation of the phenomenon of various postbuckling equilibrium paths for the functionally graded plate for different signs of imperfection with the same absolute magnitude $\left|\zeta_1^*\right|$. In particular, it can be seen for $N / N_{cr} = \sigma / \sigma_{cr} < 1.3$.

4. Conclusions

The analytical and numerical investigations on FGM – a relatively novel material, applications in plate and shell structures are presented. The effect of gradually varying volume fraction of constituent materials leads to continuous change from one surface to another eliminating interface problems and gives smooth material properties of final composite which is especially import in thermal environment applications.

An influence of imperfection values on various postbuckling equilibrium paths of the FG plate has been analyzed. The basis to explain the discussed behaviour is the nonlinear Koiter's theory of conservative systems. In the case of the FG plate, nonzero first-order sectional inner forces that cause an occurrence of nonzero postbuckling coefficients are responsible for the system sensitivity to imperfection. It results in the fact that postbuckling equilibrium paths of plate structures made of FGMs are unsymmetrically stable. This explains the observed differences in plate response dependence on imperfections sign (sense).

References

1. Birman V, Byrd LW. Modeling and analysis of functionally materials and structures. Applied Mechanics Review, 60, 2007, 195-216.
2. Bodaghi M, Saidi AR. Levy-type solution for buckling analysis of thick functionally graded rectangular plates based on the higher-order shear deformation plate theory. Applied Mathematical Modeling 2010; 34:3659-73.
3. Byskov E, Hutchinson JW. Mode interaction in axially stiffened cylindrical shells. AIAA J 1977;15(7):941-48.
4. Hui-Shen S. Functionally graded materials - Nonlinear analysis of plates and shells. CRC Press, Taylor & Francis, London; 2009.

5. Jones RM. Mechanics of Composite Materials. 1999; 2nd ed. Taylor & Francis, London.
6. Koiter WT. General theory of mode interaction in stiffened plate and shell structures. WTHD Report 590, Delft; 1976 p.41.
7. Koiter WT, Pignataro M. An alternative approach to the interaction between local and overall buckling in stiffened panels. In: Buckling of Structures Proc. of IUTAM Symposium, Cambridge; 1974 p.133-48.
8. Kolakowski Z, Krolak M. Modal coupled instabilities of thin-walled composite plate and shell structures. Composite Structures 2006. 76:303-13.
9. Kolakowski Z, Kowal-Michalska K. (Eds.) Selected problems of instabilities in composite structures. A Series of Monographs, Technical University of Lodz, Poland. 1999.
10. Kolakowski Z, Kubiak T. Load-carrying capacity of thin-walled composite structures. Composite Structures 2005; 67:417-26.
11. Kolakowski Z, Mania JR. Semi-analytical method versus the FEM for analysis of the local post-buckling. Composite Structures 2013; 97:99-106.
12. Kolakowski Z. A semi-analytical method for the analysis of the interactive buckling of thin-walled elastic structures in the second order approximation. Int. J. Solids Structures 1996. Vol.33, No.25, p. 3779-90.
13. Kolakowski Z, Krolak M, Kowal-Michalska K. Modal interactive buckling of thin-walled composite beam–columns regarding distortional deformations. Int. J. Eng. Sci, 1999; 37: 1577–96.
14. Kowal-Michalska K, Mania RJ. Static and dynamic buckling of FGM plates under compressive loading. Proceedings ICCES'11 Conference, Nanjing. 2011.
15. Kyung-Su Na, Ji-Hwan Kim. Volume fraction optimization of functionally graded composite panels for stress reduction and critical temperature. Finite Elements in Analysis and Design 2009; 45: 845-51.
16. Naderi A, Saidi AR. On pre-buckling configuration of functionally graded Mindlin rectangular plates. Mechanics Research Com. 2010; 37: 535-8.
17. Panda Satyajit, Ray MC. Nonlinear finite element analysis of functionally graded plates integrated with patches of piezoelectric fiber reinforced composite. Finite Elements in Analysis and Design. 2008; 44: 493-504.
18. Casciaro R. An introduction to the computational asymptotic post-buckling analysis of slender elastic structures. University of Calabria, Italy. Department of Mechanical Engineering - Laboratory for Mechanics of Materials Graduate Course. 2001.
19. Reddy JN. Analysis of functionally graded plates. Int. J. Numer. Meth. Eng 2000; 47: 663-84.
20. Reddy JN. Mechanics of laminated composite plates and shells. CRC Press, London, 2004.
21. Samsam Shariata BA, Javaherib R BA, Eslami BA. Buckling of imperfect functionally graded plates under in-plane compressive loading. Thin-Walled Structures 2005; 43:1020-36.
22. Singha MK, Prakash T, Ganapathi M. Finite element analysis of functionally graded plates under transverse load. Finite Elements in Analysis and Design 2011; 47: 453-60.
23. Sohn K-J, Kim J-H. Structural stability of functionally graded panels subjected to aero-thermal loads, Composite Structures, 82, 2008, 317-325.
24. Tsung-Lin Wu, Shukla KK, Jin H Huang. Post-buckling analysis of functionally graded rectangular plates. Composite Structures 2007; 81: 1-10.
25. van der Heijden AMA. WT Koiter's Elastic Stability of Solids and Structures. (Proceedings of the Internation.) Cambridge University Press 1st edition. 2008.
26. Zagari G. Koiter's asymptotic numerical methods for shell structures using a corotational formulation. PhD Thesis Universitua della Calabria 2009. Dottorato di Ricerca in Meccanica Computazionale, XXII ciclo, Settore scientifico disciplinare ICAR-08.
27. Zhou D-G, Zhou Y-H. A theoretical analysis of FGM thin plate based on physical neutral surface. Computational Material Science 2008; 44: 716-20.

Zbigniew KOLAKOWSKI
Radosław J. MANIA
Jan GRUDZIECKI
Lodz University of Technology TUL
Department of Strength of Materials (K12)
PL - 90-924 Lodz, ul. Stefanowskiego 1/15, Poland
E-mail: zbigniew.kolakowski@p.lodz.pl

Appendix

The prebuckling solution to the FG plate consisting of homogenous fields is assumed as (see Eq. (17) in [8]):

$$\begin{aligned} u^{(0)} &= (\ell / 2 - x)\Delta \\ v^{(0)} &= y\Delta A_{12} / A_{22} \\ w^{(0)} &= 0 \end{aligned} \tag{A1}$$

where Δ is the actual loading. This loading of the zero state is specified as a product of the unit loading and the scalar load factor.

Taking into account relationship (5), inner sectional forces of the prebuckling (i.e., unbending) state for the assumed homogeneous field of displacements (A1) are expressed by the following relationships before the redistribution of forces in the plate due to plate deformations:

$$\begin{aligned} N_x^{(0)} &= -(A_{11} - A_{12}^2 / A_{22})\Delta \\ N_y^{(0)} &= 0 \\ N_{xy}^{(0)} &= 0 \\ M_x^{(0)} &= -(B_{11} - B_{12}A_{12} / A_{22})\Delta \\ M_y^{(0)} &= -(B_{12} - B_{22}A_{12} / A_{22})\Delta \\ M_{xy}^{(0)} &= 0 \end{aligned} \tag{A.2}$$

The assumed displacement field and the field of inner forces, corresponding to it for the prebuckling state, fulfil equilibrium equations for the zero state as an identity.

The omission of the displacements of the fundamental state implies that we ignore the difference between the configuration of the non-deformed state and the fundamental state and we may consequently regard the previously defined displacements $u^{(0)}, v^{(0)}$ as the additional ones from the fundamental state to the adjacent state.

The first order approximation, being the linear problem of stability, allows for determination of values of critical loads, buckling modes, and initial postbuckling equilibrium paths.

This publication is a result of the research works carried out within the project subsidized over the years 2011-2014 by the state funds designated for the National Science Centre (NCN UMO-2011/01/B/ST8/07441).